Normalized Decoupling −A New Approach for MIMO Process Control System Design

Wen-Jian Cai,* Wei Ni, Mao-Jun He, and Cheng-Yan Ni

School of Electrical and Electronic Engineering, Nanyang Technological University, Singapore 639798

In this paper, a novel engineering oriented decoupling control system design method for two-input, two-output processes is presented. By employing the concept of integrated error, gain and phase changes of a transfer function when other loops are closed can be uniquely determined. Consequently, an equivalent transfer function matrix for a closed-loop control system can be obtained and its relations with the original process transfer function matrix are derived. On the basis of the equivalent transfer function matrix, parameters of a stable, proper, and causal ideal diagonal decoupler can then be easily determined by proper parameter assignments of the decoupled transfer function matrix elements. The method avoids the drawbacks of existing decoupling schemes, is very simple and can be easily understood, and can be implemented by field control engineers. An industrial process is employed to demonstrate its simplicity in design and effectiveness in control system performance.

1. Introduction

For easier field implementation, control engineers often use well established single loop PID controller tuning technologies for multi-input multioutput (MIMO) processes.[1−3] The reasons for such a practice are mainly attributed to their effectiveness and relatively simple structure, which can be easily understood and implemented. However, MIMO processes are much more difficult to control compared with single-input single multioutput (SISO) counterparts because of the existence of interactions between input and output variables. Adjusting controller parameters of one loop affects the performance of the others, sometimes to the extent of destabilizing the entire system. According to the interaction characteristics and control system requirements, one of the two PID based control schemes, i.e., decentralized or decoupling controls can be adopted. For those processes that are closely coupled and/or require being tightly controlled, decoupling control schemes are often employed to first eliminate the effect of the undesirable cross-couplings such that the process can be treated as multisingle loops and less-conservative single loop PID control design methods can be directly applied.

The theory of decoupling control for MIMO processes has been well-established. Several decoupling schemes were developed during past 30 years for two-input two-output (TITO) systems and have been well-summarized in many literature and process control textbooks (see for example 4−19 and references therein). To illustrate the pros and cons of existing decoupling control schemes, a block diagram for decoupling control structure of TITO processes is depicted in Figure 1, where $G(s) = [g_{ij}(s), (i, j = 1, 2)]$, $G_I(s) = [g_{Iij}(s), (i, j = 1, 2)]$, and $G_c(s) = \mathrm{diag}[g_{c1}(s), g_{c2}(s)]$ are two-dimensional process, decoupler, and controller transfer function matrices, respectively. The introduction of the additional transfer function block (decoupler matrix) $G_I(s)$ between the diagonal controller$G_c(s)$and the process $G(s)$, is to act upon the process $G(s)$ such that the decoupled process transfer function matrix

$$G_R(s) = G(s)G_I(s) \tag{1}$$

looking from the controller output is diagonal. In the ideal case, the decoupler causes the control loops to act as if they are totally independent of one another, thereby reducing the controller tuning task to that of tuning two noninteracting controllers.

There are three types of dynamic decoupling control schemes currently available, i.e., ideal decoupling, simplified decoupling, and inverted decoupling. The ideal decoupling scheme specifies the decoupled process transfer function matrix, $G_R(s)$, in diagonal form, then determine $G_I(s)$ by

$$G_I(s) = G^{-1}(s)G_R(s) \tag{2}$$

The method provides great convenience for the controller design since the decoupled process transfer function matrix can be specified as simple forms. However, it may result in a very complex decoupler matrix $G_I(s)$; model reduction in decoupler elements are often necessary before it can be implemented.

On the other hand, the simplified decoupling scheme has a simple decoupler form

$$G_I = \begin{bmatrix} 1 & g_{I,12} \\ g_{I,21} & 1 \end{bmatrix} = \begin{bmatrix} 1 & -g_{11}/g_{12} \\ -g_{21}/g_{22} & 1 \end{bmatrix} \tag{3}$$

The problem is that the decoupled process transfer matrix, G_R, may be complicated; the controller cannot be directly designed without introducing model reductions. In addition, the stability of G_I can not be guaranteed as the decoupler is obtained directly from the ratio of the original transfer function matrix elements.

The inverted decoupling structure, also named feedforward decoupling control, on the other hand, avoids the disadvantage of the simplified decoupling and achieves the purpose of the ideal decoupling. By assigning

$$u_1(s) = v_1(s) - u_2(s)g_{I,12}(s)$$

$$u_2(s) = v_2(s) - u_1(s)g_{I,21}(s)$$

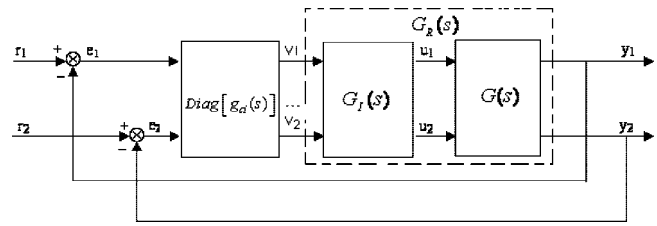

Figure 1. Block diagram of decoupling control system.

* Corresponding author. Tel: 65 6790 6862. Fax: 65 6793 3318. E-mail: ewjcai@ntu.edu.sg.

10.1021/ie8006165 CCC: $40.75
Published on Web 08/27/2008

the decoupler, G_I, has the form of exactly inverse of simplified decoupling scheme

$$G_I = \begin{bmatrix} 1 & g_{I,12} \\ g_{I,21} & 1 \end{bmatrix}^{-1} = \begin{bmatrix} 1 & -g_{11}/g_{12} \\ -g_{21}/g_{22} & 1 \end{bmatrix}^{-1} \quad (4)$$

Nevertheless, it suffers the same stability problem as the simplified decoupling scheme since the decoupler elements are determined directly by the ratio of the original transfer function matrix elements.

In this paper, a novel decoupling control scheme, "normalized decoupling control", is proposed that provides a simple alternative for design of decoupling control systems for practical control engineers. Because many processes with more than two inputs/outputs can be treated as several two-input two-output (TITO) subsystems in practice, we will concentrate our attention on the TITO process. In this scheme, the design of decoupling control systems includes three steps: (1) using the concepts of normalized integrated error (NIE) to obtain the relative normalized gain array (RNGA) and relative average residence time array (RARTA) for a given process transfer function matrix; (2) using the information obtained in the first step to obtain an equivalent transfer function (ETF) matrix and thereby the optimal approximation of the inverse for the process transfer function matrix; and (3) designing a decoupler by proper parameter selection of decoupled transfer function matrix G_R, which guarantees its stability, causality, and properness. The performance of the overall control system is compatible to those of the other decoupling control schemes, but the design method is simple, straightforward, and easy to be applied by field control engineers. A TITO industrial process is employed to demonstrate

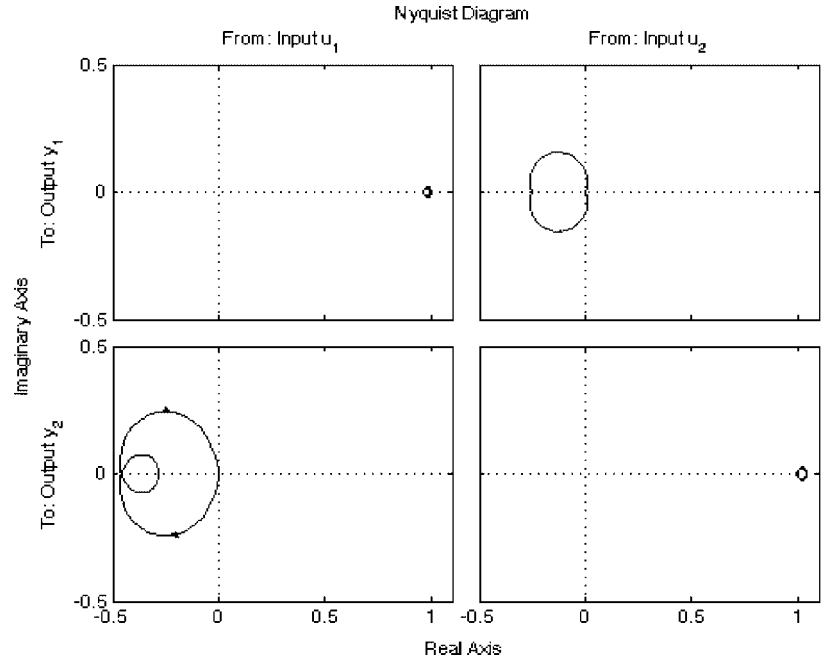

Figure 2. Nyquist Diagram of $G(s)\hat{G}^T(s)$.

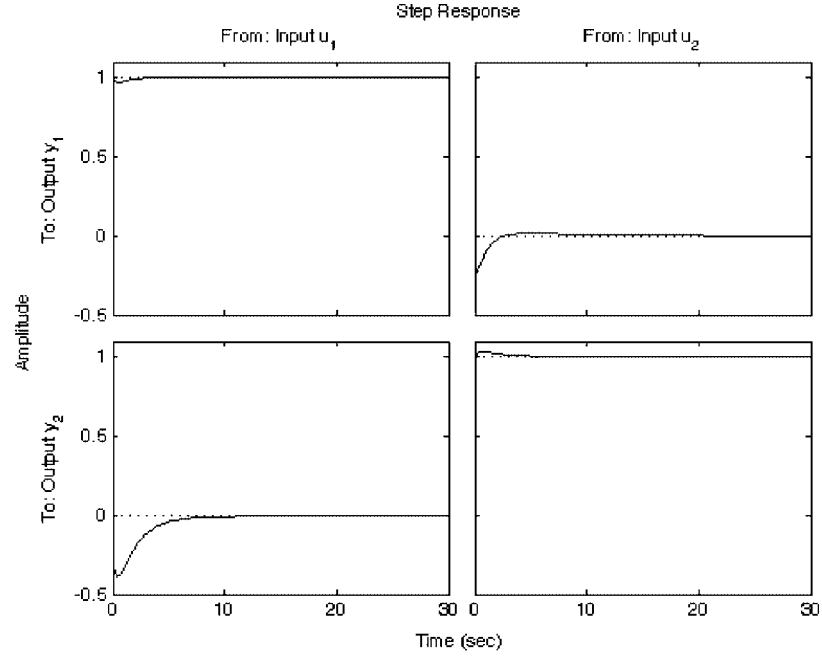

Figure 3. Step response of $\tilde{y}(s) = G(s)\hat{G}^T(s)\tilde{u}(s)$.

the advantages of the method in terms of simplicity in design and effectiveness in control system performance.

2. Equivalent Transfer Function

Because almost all industry processes are open loop stable and exhibit nonoscillatory behavior for unit step inputs, higher-order transfer function elements can be simplified by either analytical or empirical methods[20,21] to a first-order plus time delay (FOPTD) model for interaction analysis and control system design. Without loss of generality, we assume all process transfer function elements, its output response in time domain to a unit step input can be described by

$$g_{ij}(s) = \frac{k_{ij}}{\tau_{ij}s + 1} e^{-\theta_{ij}s} \tag{5}$$

and

$$y_i(t) = \begin{cases} 0 & t < \theta_{ij} \\ k_{ij} \times \bar{y}_i(t) & t \geq \theta_{ij} \end{cases} \tag{6}$$

respectively, where k_{ij} and $\bar{y}_i(t) = y_i(t)/k_{ij}$ are the steady state gain and the normalized open-loop process output, respectively, and

$$\bar{y}_i(t) = (1 - e^{-(t-\theta_{ij})/\tau_{ij}}) \tag{7}$$

To evaluate the dynamic properties of each transfer function element, let us adopt the integrated error (IE) concept by defining the normalized IE (NIE), σ, as the difference between the normalized open-loop process output and unit step input u_j. Mathematically, it can be expressed by

$$\sigma_{ij} = \int_0^\infty [u_j(t) - \bar{y}_i(t)]\, dt \tag{8}$$

Obviously, the smaller the value of σ, the better the dynamic response of the process.

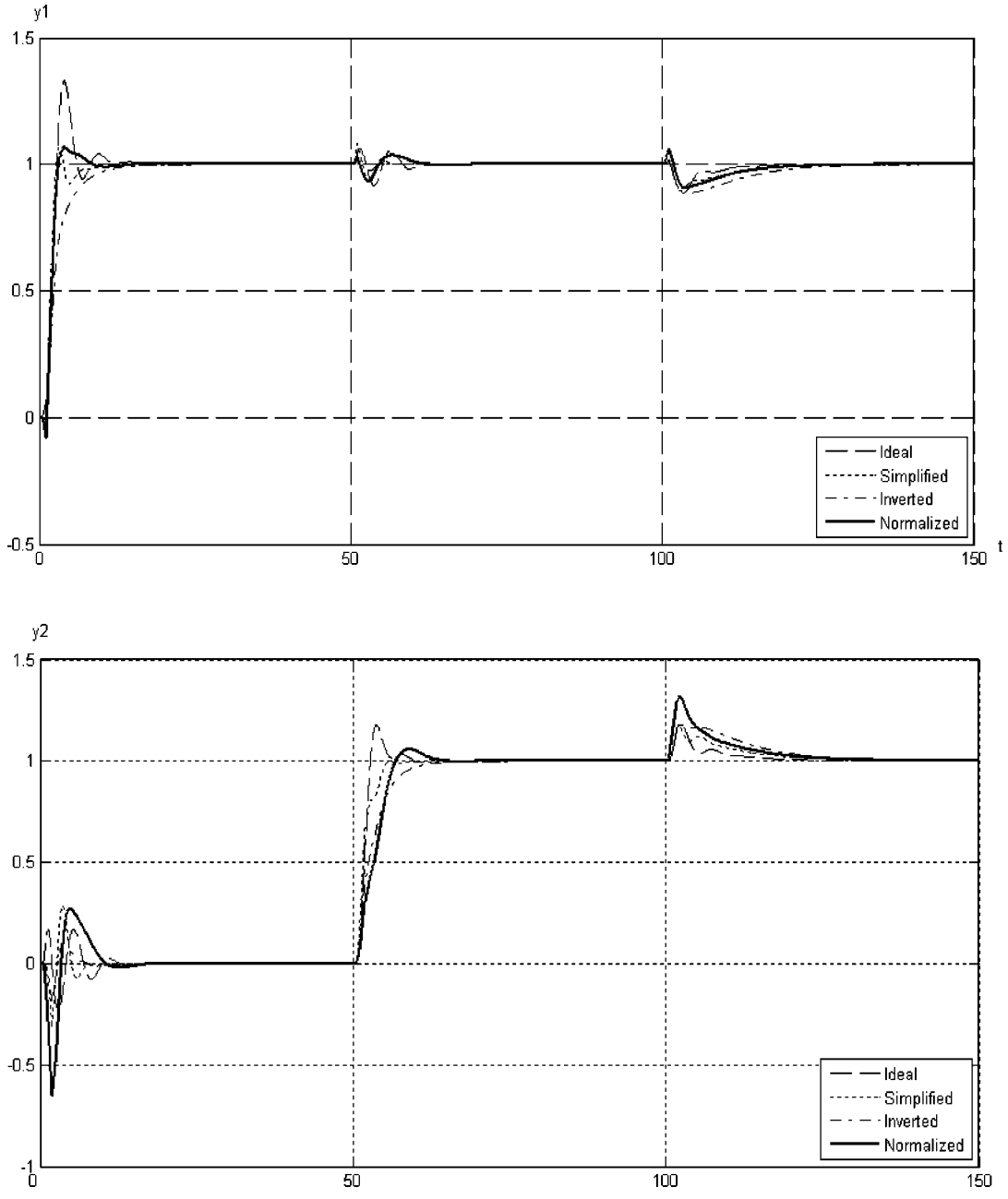

Figure 4. Output responses to step inputs.

For the normalized output response of eq 7, the solution of eq 8 is

$$\sigma_{ij} = \tau_{ij} + \theta_{ij} \tag{9}$$

which is the average residence time of loop $i-j$.

In control system design, two parameters are most important in describing the dynamic properties of a transfer function, i.e.:

• Steady state gain g_{ij} ($j0$): the steady state gain reflects the effect of the manipulated variable u_j to the controlled variable y_i;

• Average residence time σ_{ij}: the average residence time is accountable for the response speed of the controlled variable y_i to manipulated variable u_j.

To measure the interaction effects, we define the normalized gain, $k_{N,ij}$, for a particular transfer function, $g_{ij}(s)$, as[22]

$$k_{N,ij} \triangleq \frac{k_{ij}}{\sigma_{ij}} = \frac{k_{ij}}{\tau_{ij} + \theta_{ij}} \quad i,j = 1,2 \tag{10}$$

For the whole system, it can be written in a matrix form, "normalized gain matrix"

$$K_N = \begin{bmatrix} k_{N,11} & k_{N,12} \\ k_{N,21} & k_{N,22} \end{bmatrix}$$

Similar to RGA, we can define normalized relative gain between output variable y_i and input variable u_j,ϕ_{ij}, as the ratio of two normalized gains

$$\varphi_{ij} = \frac{k_{N,ij}}{\hat{k}_{N,ij}} \quad i,j = 1,2 \tag{11}$$

where $\hat{k}_{N,ij}$ is the normalized gain between output variable y_i and input variable u_j when all other loops are closed. When the effective relative gains are calculated for all the input/output combinations of a multivariable process, it results in an array of the form similar to RGA, relative normalized gain array (RNGA).

$$\Phi = \begin{bmatrix} \varphi_{11} & \varphi_{12} \\ \varphi_{21} & \varphi_{22} \end{bmatrix} \tag{12}$$

which can be calculated by

$$\Phi = K_N \otimes K_N^{-T} \tag{13}$$

where the operator $\otimes$ is the hadamard product.

The relative normalized gain reflects the combined changes in both steady state and dynamic when all other loops are open and when all other loops are closed, to separate the two changes, we first define the relative average residence time, γ_{ij}, as the ratio of loop y_i-u_j average residence time between when other loops are closed and when other loops are open, i.e.

$$\gamma_{ij} \triangleq \frac{\hat{\sigma}_{ij}}{\sigma_{ij}} \quad i,j = 1,2 \tag{14}$$

Using the definition of RNGA, we can rewrite eq 11 as

$$\hat{k}_{ij} \times \sigma_{ij} = \frac{k_{ij} \times \hat{\sigma}_{ij}}{\varphi_{ij}} \quad i,j = 1,2 \tag{15}$$

where $\hat{\sigma}_{ij}$ is the average residence time of loop $i-j$ when other loops are closed. Equation (15) provides both gain and average residence time change information when all other loops are closed.

To separate these two changes, we first use the definition of RGA[23]

$$\hat{k}_{ij} = \frac{k_{ij}}{\lambda_{ij}} \quad i,j = 1,2 \tag{16}$$

where λ_{ij} can be calculated by eq 13 by letting $\sigma_{ij} = 1$. Then, substitute eq 16 into eq 15 and rearrange, and we obtain a formula for calculating γ_{ij}

$$\gamma_{ij} = \frac{\hat{\sigma}_{ij}}{\sigma_{ij}} = \frac{\varphi_{ij}}{\lambda_{ij}} \quad i,j = 1,2 \tag{17}$$

When the relative average residence times are calculated for all the input/output combinations of the TITO process, it results in an array of the form, i.e., relative average residence time array (RARTA) defined as

$$\Gamma = \begin{bmatrix} \gamma_{11} & \gamma_{12} \\ \gamma_{21} & \gamma_{22} \end{bmatrix} \triangleq \Phi \odot \Lambda = \begin{bmatrix} \varphi_{11} & \varphi_{12} \\ \varphi_{21} & \varphi_{22} \end{bmatrix} \odot \begin{bmatrix} \lambda_{11} & \lambda_{12} \\ \lambda_{21} & \lambda_{22} \end{bmatrix} \tag{18}$$

where the operator $\odot$ is the hadamard division.

Because the relative average residence time is the ratio of the average residence times between when other loops are closed and when other loops are open, $\hat{\sigma}_{ij}$ represent the dynamic changes of the transfer function $g_{ij}(s)$ when other loops closed. By the definition of RARTA, we can write

$$\hat{\sigma}_{ij} = \gamma_{ij} \times \sigma_{ij} = \gamma_{ij} \times \tau_{ij} + \gamma_{ij} \times \theta_{ij} \quad i,j = 1,2 \tag{19}$$

The average resident time of loop $i-j$th when other loops are closed is the open loop average resident time scaled by a factor γ_{ij}.

In process control, steady state gain, time constant, and time delay are the parameters that are uppermost for control system design. By using RGA and RARTA information, gain and phase changes of a transfer function element when other loops closed can be uniquely determined. That is: A transfer function element of a MIMO process when other loops are closed can be approximated by a transfer function element having the same form as the open-loop transfer function element, but the steady state gain, time constant and time delay are scaled by $1/\lambda_{ij}$ and γ_{ij}, respectively, i.e.

$$\hat{g}_{ij}(s) = \hat{k}_{ij} \times \frac{1}{\hat{\tau}_{ij}s + 1} e^{-\hat{\theta}_{ij}s} = \frac{k_{ij}}{\lambda_{ij}} \times \frac{1}{\gamma_{ij}\tau_{ij}s + 1} e^{-\gamma_{ij}\theta_{ij}s} \quad i,j = 1,2 \tag{20}$$

$\hat{g}_{ij}(s)$ in eq 20 is the equivalent transfer function (ETF) of loop $i-j$ when other loops are closed, which is optimal under IE criterion. Therefore, $\hat{g}_{ij}(s)$ should resemble the dynamic response of corresponding true transfer function element when other loops are closed.

Now define

$$\hat{G}(s) \triangleq \begin{bmatrix} 1/\hat{g}_{11}(s) & 1/\hat{g}_{12}(s) \\ 1/\hat{g}_{21}(s) & 1/\hat{g}_{22}(s) \end{bmatrix} \tag{21}$$

as the ETF matrix, where each element is the inverse of corresponding ETF. Because the main difficulty for design of ideal decoupler is the inverse of process matrix, $G(s)$, we will develop the relations between inverse of process matrix, $G(s)$,

Table 1. Typical Gain and Phase Margin Values

$A_{m,ii}$	$\Phi_{m,ii}$	k_{ii}
2	$\pi/4$	$\pi/4L_{R,ii}k_{R,ii}$
3	$\pi/3$	$\pi/6L_{R,ii}k_{R,ii}$
4	$3\pi/8$	$\pi/8L_{R,ii}k_{R,ii}$
5	$2\pi/5$	$\pi/10L_{R,ii}k_{R,ii}$

and the ETF matrix of eq 21 which is the foundation of the normalized decoupling scheme.

3. Relation Between ETF and Process Transfer Function Matrices

Using the original definition of DRGA[24,25]

$$\lambda_{ij}(s)=\frac{\left[\int_0^{\omega_{c,ij}}(\partial y_i/\partial u_j)\,d\omega\right]_{\text{all loops open}}}{\left[\int_0^{\omega_{c,ij}}(\partial y_i/\partial u_j)\,d\omega\right]_{\text{all other loops closed except for loop } y_i-u_j}}=\frac{g_{ij}(s)}{\hat{g}_{ij}(s)} \quad (22)$$

for each element in $\Lambda(s)$, we have

$$\Lambda(s)=\begin{bmatrix} g_{11}(s)/\hat{g}_{11}(s) & g_{12}(s)/\hat{g}_{12}(s) \\ g_{21}(s)/\hat{g}_{21}(s) & g_{22}(s)/\hat{g}_{22}(s)\end{bmatrix}$$

which is

$$\Lambda(s)=G(s)\otimes\hat{G}(s)=\begin{bmatrix} g_{11}(s) & g_{12}(s) \\ g_{21}(s) & g_{22}(s)\end{bmatrix}\otimes\begin{bmatrix} 1/\hat{g}_{11}(s) & 1/\hat{g}_{12}(s) \\ 1/\hat{g}_{21}(s) & 1/\hat{g}_{22}(s)\end{bmatrix} \quad (23)$$

Using RNGA of eq 12, we can derive an important relation, i.e.:

$$G^{-1}(s)=\hat{G}^T(s) \quad (24)$$

or equivalently

$$G(s)\hat{G}^T(s)=I \quad (25)$$

The detailed derivation of eq 25 is given in the Appendix.

The following example is employed to illustrate that eqs 24 or 25 indeed hold.

Example 1. The VL column system with its transfer function matrix was given by Luyben[26]

$$G(s)=\begin{bmatrix} \dfrac{-2.2e^{-s}}{7s+1} & \dfrac{1.3e^{-0.3s}}{7s+1} \\ \dfrac{-2.8e^{-1.8s}}{9.5s+1} & \dfrac{4.3e^{-0.35s}}{9.2s+1}\end{bmatrix}$$

A simple calculation gives

$$K=\begin{bmatrix}-2.2 & 1.3\\ -2.8 & 4.3\end{bmatrix},\quad K_N=\begin{bmatrix}-0.2750 & -0.1781\\ -0.2478 & -0.4503\end{bmatrix}$$

and

$$\Lambda=K\otimes K^{-T}=\begin{bmatrix}1.6254 & -0.6254\\ -0.6254 & 1.6254\end{bmatrix}$$

$$\Phi=K_N\otimes K_N{}^{-T}=\begin{bmatrix}1.5537 & -0.5537\\ -0.5537 & 1.5537\end{bmatrix}$$

$$\Gamma=\Phi\odot\Lambda=\begin{bmatrix}0.9558 & 0.5532\\ 0.8852 & 0.9558\end{bmatrix}$$

which results in the following ETF parameters

$$\hat{K}=K\odot\Lambda=\begin{bmatrix}-1.3534 & -2.0785\\ 4.4769 & 2.6454\end{bmatrix}$$

$$\hat{T}=\Gamma\otimes T=\begin{bmatrix}6.6910 & 6.1970\\ 8.4103 & 8.7939\end{bmatrix}$$

$$\hat{L}=\Gamma\otimes L=\begin{bmatrix}0.9558 & 0.2655\\ 1.5935 & 0.3345\end{bmatrix}$$

Substituting these ETF parameters into the original transfer function matrix, the ETF matrix is obtained as

$$\hat{G}^T(s)=\begin{bmatrix}\dfrac{6.6910s+1}{-1.3534}e^{0.9558s} & \dfrac{8.4103s+1}{4.4769}e^{1.5935s}\\ \dfrac{6.1970s+1}{-2.0785}e^{0.2655s} & \dfrac{8.7939s+1}{2.6454}e^{0.3345s}\end{bmatrix}$$

The relation of $G(s)\hat{G}^T(s)=I$ is verified by both frequency domain and time domain methods:

- The Nyquist plot $G(s)\hat{G}^T(s)$ is shown in Figure 2;
- The step response of $\tilde{y}(s)=G(s)\hat{G}^T(s)\tilde{}\,u(s)$ is shown in Figure 3.

The simulation result clearly demonstrated that even though the results have some small deviations from that of identity matrix's, they are close enough to consider that the relation of eq 24 or 25 holds.

4. Decoupler Parametrization

Using ETF matrix to replace the inverse of the process transfer matrix, and substituting eq 22 into eq 2, the design of

Table 2. Difference Decoupling Schemes for Example 2

decoupling method matrix	G_R	$G_I(s)$	$G_c(s)$ $A_{m,i}=3db$ $\Phi_{m,i}=\pi/3$rad
ideal $D(s)$ = [1 and 0 0 & $e^{-0.7s}$]	$g_{R,11}=-2.2e^{-s}/(7s+1)$	$g_{I11}=g_{I22}=(89.87s+9.46)/(25.116s^2+59.112s+5.82)$	$g_{c1}(s)=-1.6660-0.2380/s$
	$g_{R,22}=4.3e^{-1.05s}/(9.2s+1)$	$g_{I12}=(53.105s+5.59)/(25.116s^2+59.112s+5.82)$ $g_{I21}=(-42.504s^2+52.052s+6.16)/(25.116s^2+59.112s+5.82)$	$g_{c2}(s)=1.0669+0.1160/s$
simplified $D(s)$ = [1 and 0 0 & $e^{-0.7s}$]	$g_{R11}(s)\approx-1.3535e^{-1.01s}/(7.31s+1)$	$g_{I1}=0.5909$	$g_{c1}(s)=-2.7999-0.3830/s$
	$g_{R22}(s)\approx2.6455e^{-1.06s}/(9.52s+1)$	$g_{I2}=(5.9907s+0.6512)e^{-0.75s}/9.5s+1)$	$g_{c2}(s)=1.7775+0.1867/s$
inverted $N_x=e^{\theta_{12}}-\theta_{11}=e^{-0.7s}$	$g_{R11}(s)\approx-1.3535e^{-1.01s}/(7.31s+1)$	$g_{I1}=0.5909$	$g_{c1}(s)=-1.6660-0.2380/s$
	$g_{R22}(s)\approx2.6455e^{-1.06s}/(9.52s+1)$	$g_{I2}=(5.9907s+0.6512)e^{-0.75s}/(9.5s+1)$	$g_{c2}(s)=1.0669+0.1160/s$
normalized	$g_{R,11}=2.0785e^{-0.9558s}/(6.6910s+1)$	$g_{I,11}=-1.5357$	$g_{c1}=1.7633+0.2635/s$
	$g_{R,22}=4.4769e^{-1.5935s}/(8.7939s+1)$	$g_{I,12}=(8.4103s+1)/(8.7939s+1)$ $g_{I,21}=(-6.1970s+1)e^{-0.6903s}/(6.6910s+1)$ $g_{I,22}=1.6923e^{-1.2590s}$	$g_{c2}=0.6454+0.0734/s$

Table 3. IAE Values for Each Decoupling Scheme

	ideal		simplified		inverted		normalized	
	loop 1	loop 2	loop 1	loop 2	loop 1	loop 2	loop 1	loop 2
tracking	2.770	0.971	2.802	0.811	3.153	0.440	2.273	2.068
interaction	0.364	2.253	0.179	2.076	0.091	3.308	0.313	3.567
disturbance	0.546	0.926	0.883	1.510	1.411	2.432	0.917	2.276

normalized decoupler starts from the obtained $\hat{G}^T(s)$, determines the diagonal forward transfer function matrix $G_R(s)$, such that the decoupler $G_I(s)$

$$G_I(s) = \hat{G}^T(s) G_R(s) \tag{26}$$

satisfies certain conditions for implementation.

To see how the problem definition and design procedure of normalized decoupling control system is different from the existing methods, let each element of the process transfer function matrix be represented by eq 5, ETF by eq 20, and the forward transfer function element be of the form

$$g_{R,ii}(s) = \frac{k_{R,ii}}{\tau_{R,ii}s + 1} e^{-\theta_{R,ii}s} \quad i,j = 1,2 \tag{27}$$

From eq 26, we have

$$G_I(s) = \hat{G}^T(s) G_R(s) \Rightarrow$$

$$\begin{bmatrix} g_{I,11}(s) & g_{I,12}(s) \\ g_{I,21}(s) & g_{I,22}(s) \end{bmatrix} = \begin{bmatrix} 1/\hat{g}_{11}(s) & 1/\hat{g}_{21}(s) \\ 1/\hat{g}_{12}(s) & 1/\hat{g}_{22}(s) \end{bmatrix} \times \begin{bmatrix} g_{R,11}(s) & 0 \\ 0 & g_{R,22}(s) \end{bmatrix}$$

which results in

$$\begin{bmatrix} g_{I,11}(s) & g_{I,12}(s) \\ g_{I,21}(s) & g_{I,22}(s) \end{bmatrix} = \begin{bmatrix} g_{R,11}(s)/\hat{g}_{11}(s) & g_{R,22}(s)/\hat{g}_{21}(s) \\ g_{R,11}(s)/\hat{g}_{12}(s) & g_{R,22}(s)/\hat{g}_{22}(s) \end{bmatrix} \tag{28}$$

and the decoupler design is to select $g_{R,ii}(s)$, such that $G_I(s)$ has the simplest form and is implementable.

Substituting eqs 27 and 20 into eq 28, the element of the resultant decoupler is

$$g_{I,ij}(s) = \frac{k_{R,ii}}{\hat{k}_{ji}} \times \frac{\hat{\tau}_{1,ji}s + 1}{\tau_{R,ii}s + 1} e^{-(\theta_{R,ii} - \hat{\theta}_{ji})s} \quad i,j = 1,2 \tag{29}$$

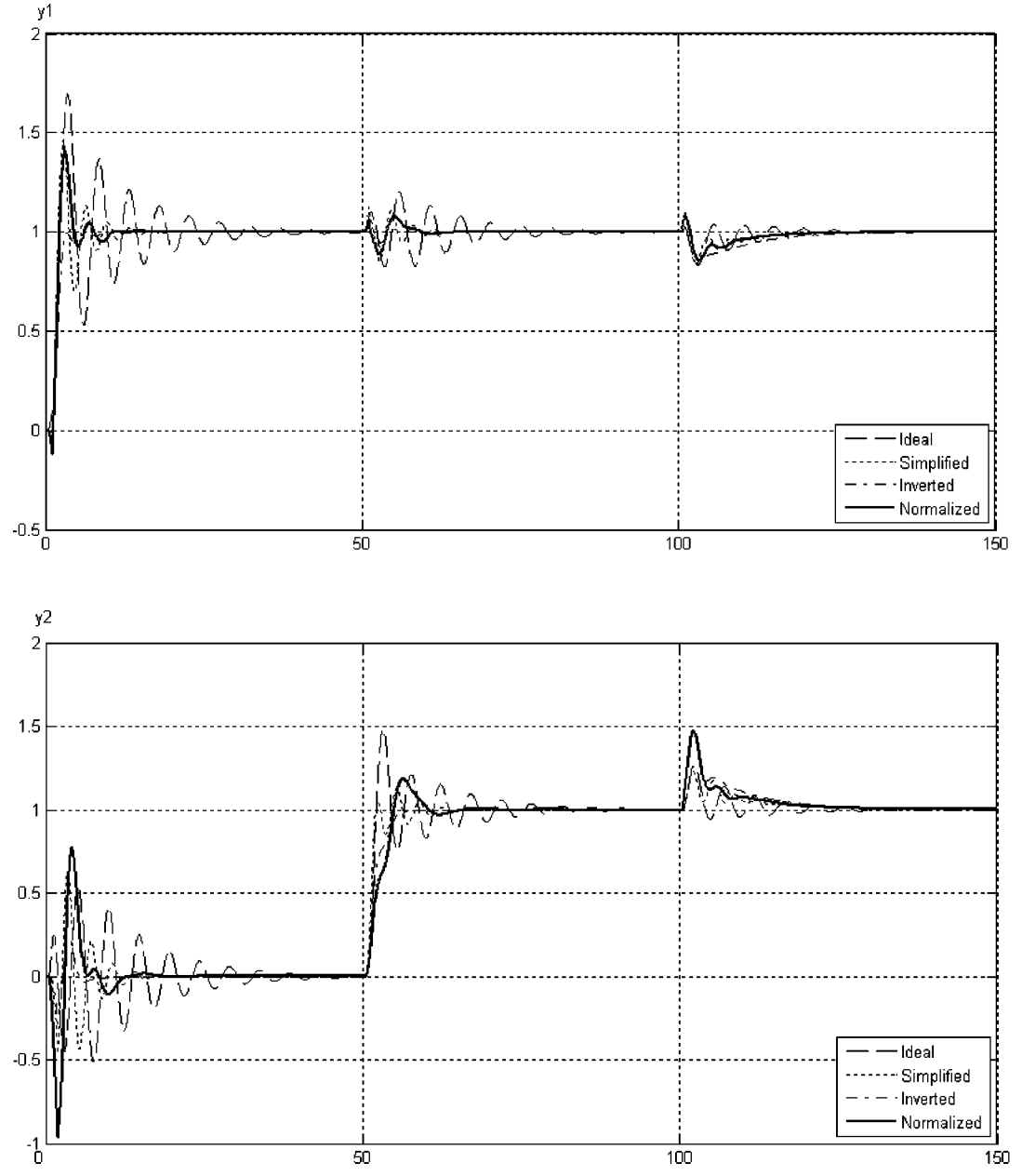

Figure 5. Robustness to steady state gain variations, $k_{ij} = 1.5 \times k_{ij}^0$ for $i, j = 1, 2$.

The design of decoupler is now to specify the parameters in $g_{R,ii}(s)$ such that eq 29 to be physically realizable; therefore, the parameters of $g_{R,ii}(s)$ must be selected to satisfy the following conditions:

1. Stability*:* The decoupler must generate bounded responses to bounded inputs; therefore all poles of $g_{R,ii}(s)$ must lie in the open left-half plane. Both dynamic properties and stability can be easily satisfied by selecting the corresponding time constant $T_{R,ii}$.

2. Properness*:* To avoid pure differentiation of signals, we must require that $g_{I,ij}(s)$ be proper or semiproper, that is, the quantity of

$$\lim_{|s|\mapsto\infty} g_{I,ij}(s) \quad i,j=1,2 \tag{30a}$$

must be finite

$$0 \le \lim_{|s|\mapsto\infty} |g_{I,ij}(s)| < \infty \quad i,j=1,2 \tag{30b}$$

This condition requires that the order of $g_{R,ii}(s)$ be higher than or equal to the orders of all$g_{I,ji}(s)$. For the given original system model, the specification of $g_{R,ii}$(s) in eq 27 already satisfies this condition.

3. Causality: $g_{I,ij}(s)$ must be causal, which means that the decoupler must not require prediction, i.e., it must rely only on the current and previous measurements. This requires that

$$(\theta_{R,ii} - \hat{\theta}_{ij}) \ge 0, \text{ for } j=1,2 \tag{31}$$

be satisfied by letting $\theta_{R,ii} = \text{Max}_{\ j\ =\ 1,2}\hat{\theta}_{ij}$.

Once $G_I(s)$ is determined, the controller $G_c(s)$ can be designed by the elements of $G_R(s)$ such that$g_{c,ii}(s)g_{R,ii}(s)$ for $i = 1, 2$, meet the control system specifications.

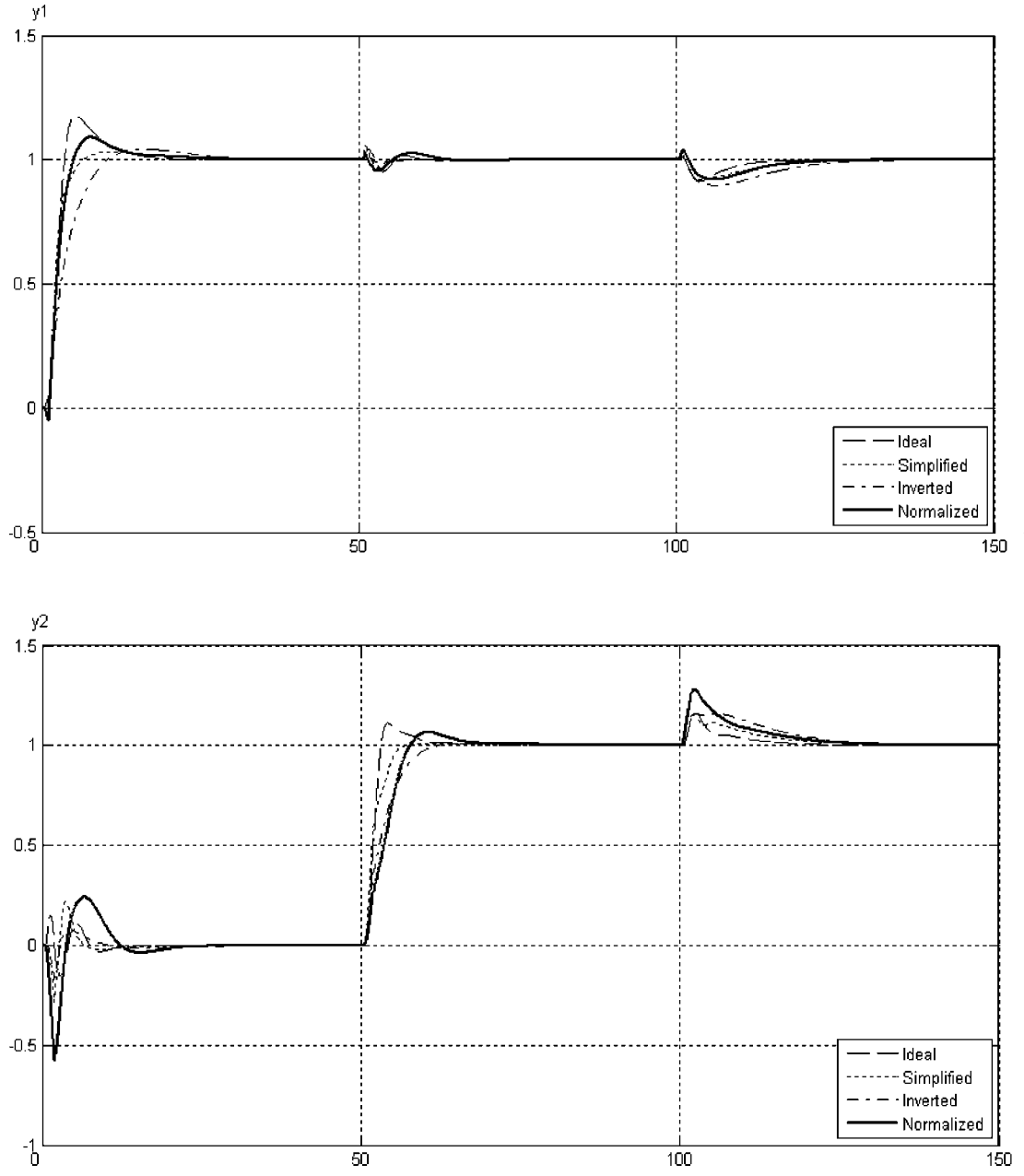

Figure 6. Robustness to time constant variations, $\tau_{ij} = 1.5 \times \tau_{ij}^0$ for $i, j = 1, 2$.

Remark 1. Comparing with the conventional ideal decoupler approaches, eq 24 provides an alternative way of finding the inverse of the process matrix by using the ETF matrix to simplify the design procedure. Because this design follows the same principles of ideal diagonal decoupling technique, the structure limitations arise from ideal diagonal decoupling control (cost in terms of sensitivity, extra nonminimum phase zeros, extra unstable poles) still need to be carefully examined.[1−3]

5. Case Studies

In this section, we apply the proposed design method to LV process to compare with the existing methods and show its effectiveness and simplicity.

Without loss of generality, we assume that each element in $G_R(s)$ from all different design methods is a first order plus dead time (FOPDT) model of eq 27, and the control is by standard PI controller of the form

$$g_{c,ii}(s) = k_{p,ii} + \frac{k_{i,ii}}{s} \quad i = 1, 2$$

Specify the open-loop transfer function be of the form

$$g_{c,ii}(s)g_{R,ii}(s) = k_{ii}\frac{k_{R,ii}}{s}e^{-L_{R,ii}s} \quad i = 1, 2 \tag{32}$$

By gain and phase margin synthesis method, the PID parameters for each loop is given by[27]

$$\begin{bmatrix} k_{p,ii} \\ k_{i,ii} \end{bmatrix} = \frac{\pi}{2A_m L_{R,ii} k_{R,ii}} \begin{bmatrix} a_{R1,ii} \\ 1 \end{bmatrix} \quad i = 1, 2 \tag{33}$$

where the gain and phase margin are interrelated to each other as shown in Table 1.

For simplicity, the gain and phase margins for all loops in all decoupling schemes are specified as $A_{m,i} = 3db$ and $\Phi_{m,i} = \pi/3$rad, respectively.

5.1. Example 1 Continued: Decoupler Design for Nominal Process. By using normalized decoupling control system design rules 1−3, the decoupled forward transfer function is selected as

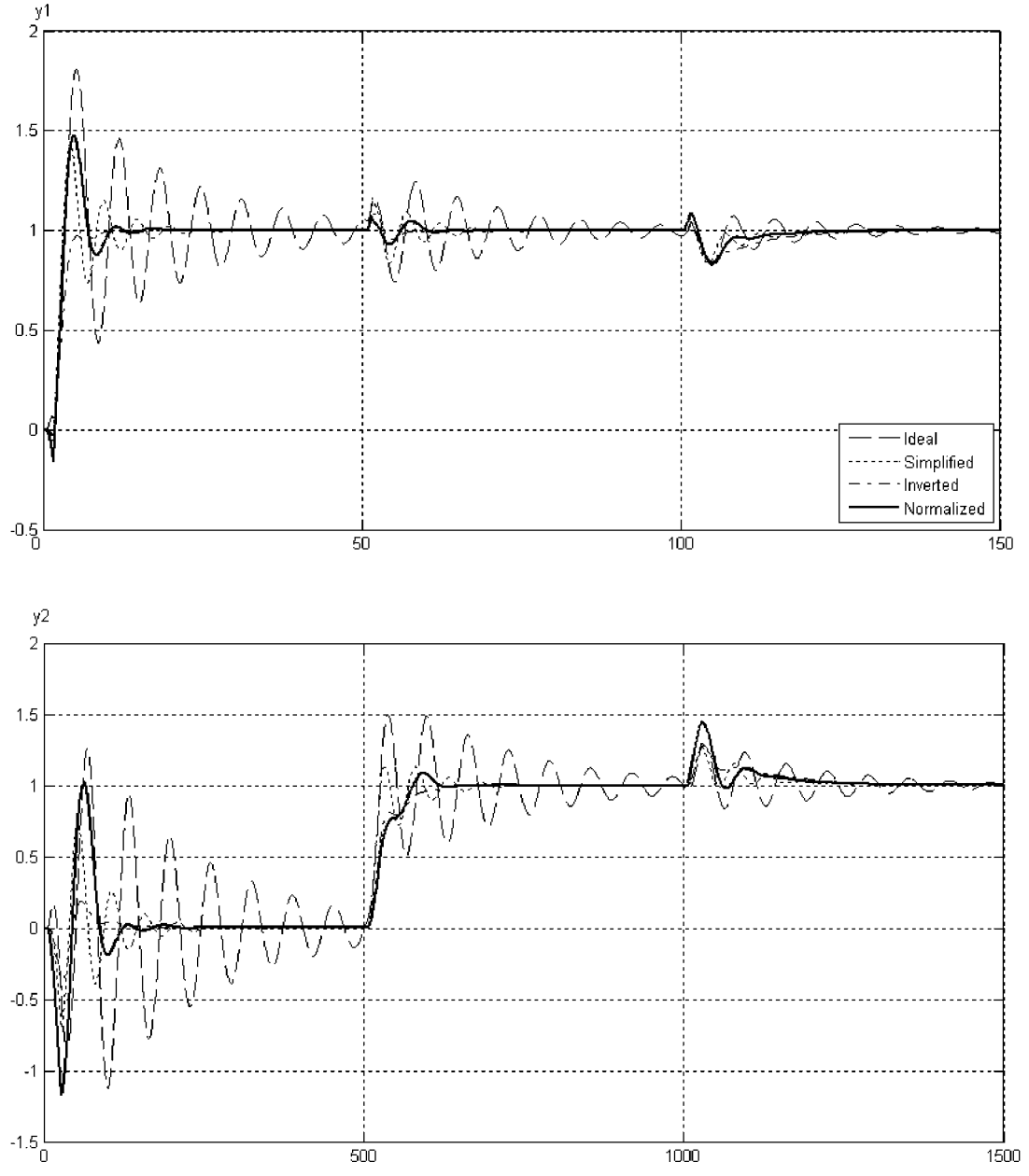

Figure 7. Robustness to time-delay variations, $\theta_{ij} = 1.5 \times \theta_{ij}^0$ for $i, j = 1, 2$.

$$G_R(s)=\begin{bmatrix}\dfrac{2.0785}{6.6910s+1}e^{-0.9558s} & 0\\ 0 & \dfrac{4.4769}{8.7939s+1}e^{-1.5935s}\end{bmatrix}$$

which gives a stable, causal, and proper decoupler

$$\widehat{G}_I(s)=\widehat{G}^T(s)G_R(s)=\begin{bmatrix}-1.5357 & \dfrac{8.4103s+1}{8.7939s+1}\\ (-1)\dfrac{6.1970s+1}{6.6910s+1}e^{-0.6903s} & 1.6923e^{-1.2590s}\end{bmatrix}$$

Using gain and phase margins method, the diagonal controller is obtained as

$$G_c(s)=\begin{bmatrix}1.7633+\dfrac{0.2635}{s} & 0\\ 0 & 0.6454+\dfrac{0.0734}{s}\end{bmatrix}$$

The resultant matrices and PI controllers of the proposed design method and other three decoupling control design methods are listed in Table 2 and the output responses are shown in Figure 4, respectively, where the unit set-points change in r_1 at $t = 0$ and r_2 at $t = 50$. To assess their disturbance rejection capabilities, a step output disturbances $d = 0.5$ at $t = 100$ is inserted in both loops. It is noted that a delay element is required in the three existing decoupling methods to make the decouplers causal, whereas it is embedded into the design process in the normalized decoupling method. The integrated absolute error (IAE) for each case is calculated and listed in Table 3.

5.2. Example 1 Continued: Investigation of Robustness. To compare the robustness of different decoupling control schemes, we mismatch the process model by increasing all 4 steady-state gains, 4 time constants, and 4 time delays by a factor of 1.5, separately, with all decouplers and controller parameters kept the same as before. The closed-loop responses are shown in Figures 5−7, respectively. It shows that under such model mismatches, the response of normalized decoupling control system exhibits better robustness than that of other design methods.

The above simulations show that the normalized decoupling control scheme is comparable to other decoupling schemes in both nominal performance and robustness, but its design procedure is much simpler and implementable decouplers can be directly designed.

6. Conclusions

In this paper, a novel decoupling control system design technique "normalized decoupling" for the TITO processes was proposed. By employing the concepts of normalized integrated error, a transfer function element can be uniquely represented by an equivalent transfer function for closed-loop control system. The relations between the equivalent transfer function matrix and the original process transfer function matrix was uniquely determined. On the basis of the equivalent transfer function matrix, criteria for determining a stable, proper, and causal ideal diagonal decoupler was established. The method is very simple, straightforward, and easy to understand by field engineers and embedded into the computer control systems. A TITO industrial process was employed to demonstrate the simplicity of the design procedure and superior control system performance compared with existing methods. For the full acceptance of the design methodology in both academia and industry worlds, however, several research topics emerged from using equivalent transfer function matrix for control system design have to be further studied, including: (1) the necessary and sufficient conditions for the existence of ideal diagonal decoupler in terms of equivalent transfer function matrix; (2) the extension of the design method to higher dimensional processes, which may involve optimal structure selection for partial decoupling; (3) the development of design procedure for process transfer function matrix with non-FOPTD model elements, e.g., those with oscillatory dynamics, inverse response or integrator; and (4) optimal selection of decoupled transfer function parameters such that the decoupler is implementable with best overall system performances.

Appendix

Because normalized relative gain is an optimal approximation of dynamic relative gain under the criterion of IE, for TITO processes, we can write

$$\varphi=\frac{g_{11}(s)}{\hat{g}_{11}(s)}=\frac{g_{22}(s)}{\hat{g}_{22}(s)}=\frac{1}{1-\dfrac{g_{12}(s)g_{21}(s)}{g_{11}(s)g_{22}(s)}} \tag{A1a}$$

and

$$1-\varphi=\frac{g_{12}(s)}{\hat{g}_{12}(s)}=\frac{g_{21}(s)}{\hat{g}_{21}(s)} \tag{A1b}$$

Substituting both$G(s)$and $\hat{G}^T(s)$ into eq (25) and refer to the Equations (A1a), we have

$$G(s)\widehat{G}^T(s)=\begin{bmatrix}\dfrac{g_{11}(s)}{\hat{g}_{11}(s)}+\dfrac{g_{12}(s)}{\hat{g}_{12}(s)} & \dfrac{g_{11}(s)}{\hat{g}_{21}(s)}+\dfrac{g_{12}(s)}{\hat{g}_{22}(s)}\\ \dfrac{g_{21}(s)}{\hat{g}_{11}(s)}+\dfrac{g_{22}(s)}{\hat{g}_{12}(s)} & \dfrac{g_{21}(s)}{\hat{g}_{21}(s)}+\dfrac{g_{22}(s)}{\hat{g}_{22}(s)}\end{bmatrix}$$

$$=\begin{bmatrix}\varphi+(1-\varphi) & \dfrac{g_{11}(s)}{\hat{g}_{21}(s)}+\dfrac{g_{12}(s)}{\hat{g}_{22}(s)}\\ \dfrac{g_{21}(s)}{\hat{g}_{11}(s)}+\dfrac{g_{22}(s)}{\hat{g}_{12}(s)} & \varphi+(1-\varphi)\end{bmatrix}$$

$$=\begin{bmatrix}1 & \dfrac{g_{11}(s)}{\hat{g}_{21}(s)}+\dfrac{g_{12}(s)}{\hat{g}_{22}(s)}\\ \dfrac{g_{21}(s)}{\hat{g}_{11}(s)}+\dfrac{g_{22}(s)}{\hat{g}_{12}(s)} & 1\end{bmatrix} \tag{A2}$$

Now, we need to show that

$$\frac{g_{11}(s)}{\hat{g}_{21}(s)}+\frac{g_{12}(s)}{\hat{g}_{22}(s)}=0 \tag{A3a}$$

and

$$\frac{g_{21}(s)}{\hat{g}_{11}(s)}+\frac{g_{22}(s)}{\hat{g}_{12}(s)}=0 \tag{A3b}$$

For eq A3a, using eqs A1a and A1b, we can obtain

$$\frac{g_{11}(s)}{\hat{g}_{21}(s)}+\frac{g_{12}(s)}{\hat{g}_{22}(s)}=\frac{g_{11}(s)\hat{g}_{22}(s)+g_{12}(s)\hat{g}_{21}(s)}{\hat{g}_{21}(s)\hat{g}_{22}(s)}$$

$$=\frac{\dfrac{g_{11}(s)g_{22}(s)}{\varphi}+\dfrac{g_{12}(s)g_{21}(s)}{1-\varphi}}{\hat{g}_{21}(s)\hat{g}_{22}(s)}$$

$$= \frac{g_{11}(s)g_{22}(s) - \varphi[g_{11}(s)g_{22}(s) - g_{12}(s)g_{21}(s)]}{\varphi(1-\varphi)\hat{g}_{21}(s)\hat{g}_{22}(s)}$$

$$= \frac{g_{11}(s)g_{22}(s) - \varphi g_{11}(s)g_{22}(s)\left[1 - \frac{g_{12}(s)g_{21}(s)}{g_{11}(s)g_{22}(s)}\right]}{\varphi(1-\varphi)\hat{g}_{21}(s)\hat{g}_{22}(s)}$$

which results in

$$\frac{g_{11}(s)}{\hat{g}_{11}(s)} + \frac{g_{12}(s)}{\hat{g}_{22}(s)} = \frac{g_{11}(s)g_{22}(s) - g_{11}(s)g_{22}(s)}{\varphi(1-\varphi)\hat{g}_{21}(s)\hat{g}_{22}(s)} = 0 \quad \text{(A4)}$$

The same derivation procedure can also be used for eq A3b.

Literature Cited

(1) Shinskey, F. G., *Process Control Systems: Application, Design, and Adjustment*, 4th ed.; McGraw-Hill: New York, 1996.

(2) Skogestad, S., Postlethwaite, I., *Multivariable Feedback Control: Analysis and Design*; John Wiley & Sons: New York, 1996.

(3) Astrom, K. J.; Hagglund T., *PID controllers: Theory, Design, And Tuning*, 2nd ed.; Instrument Society of America: Research Triangle, Park, NC, 1995.

(4) Lin, C. A., Necessary and Sufficient Conditions for Existence of Decoupling Controllers. *Proceedings of the IEEE 34th Conference on Decision and Control*, New Orleans, Dec 13−15, 1995; Institute of Electrical and Electronics Engineers: Piscataway, NJ, 1995; pp 3200−3202.

(5) Gomez, G. I.; Goodwin, G. C. An algebraic approach to decoupling in linear multivariable systems. *Int. J. Control* **2000**, *73* (7), 528–599.

(6) Wang, Q. G.; Huang, B.; and Guo, X. Auto-tuning of TITO decoupling controllers from step tests. *ISA Trans.* **2000**, *39*, 407–418.

(7) Gilbert, A. F.; Yousef, A.; Natarajan, K.; and Deighton, S. Tuning of PI controllers with one-way decoupling in 2 × 2 MIMO systems based on finite frequency response date. *J. Process Control* **2002**, *13*, 553–567.

(8) Wang, Q. G.; and Yang, Y. S. Transfer function matrix approach to decoupling problem with stability. *Syst. Control Lett.* **2002**, *47*, 103–110.

(9) Waller, M.; Waller, J. B.; Waller, K. V. Decoupling revisited. *Ind. Eng. Chem. Res.* **2003**, *42*, 4575–7.

(10) Luyben, W. L. Distillation decoupling. *AIChE J.* **1970**, *16*, 198–203.

(11) Waller, K. V. Decoupling in distillation. *AIChE J.* **1974**, *20*, 592–594.

(12) Zheng, J. C.; Guo, G. X.; and Wang, Y. Y. Feedforward decoupling control design for dual-actuator system in hard disk drives. *IEEE Trans. Magn.* **2004**, *40*, 2080–2082.

(13) Gagnon, E.; Pomerleau, A.; and Desbiens, A. Simplified, ideal or inverted decoupling? *ISA Trans.* **1998**, *37*, 265–276.

(14) Wade, H. L. Inverted decoupling: A neglected technique. *ISA Trans.* **1997**, *36*, 3–10.

(15) Ogunnaike, B. A.; Ray, W. H. Multivariable controller design for linear systems having multiple time delays. *AIChE J.* **1979**, *25*, 1043–57.

(16) Viknesh, R.; Sivakumaran, N.; Sarat, C. J.; and Radhakrishnan, T. K. A critical study of decentralized controllers for a multivariable system. *Chem. Eng. Technol.* **2004**, *27*, 880–889.

(17) Chen, P. Y.; Zhang, W. D. Improvement on an inverted decoupling technique for a class of stable linear multivariable processes. *ISA Trans.* **2007**, *46*, 199–210.

(18) Wang, Q. G. Decoupling with internal stability for unity output feedback systems. *Automatica* **1992**, *28* (2), 411–415.

(19) Wang, Q. G.; Zou, B.; Lee, T. H.; and Bi, Q. Auto-tuning of multivariable PID controllers from decentralized relay feedback. *Automatic* **1997**, *33* (3), 319–330.

(20) Skogestad, S. Simple analytic rules for model reduction and PID controller tuning. *J. Process Control* **2003**, *13*, 291–309.

(21) Bi, Q.; Cai, W. J.; et al. "Robust identification of first-order plus dead-time model from step response". *IFAC J.: Control Eng. Pract.* **1999**, *7*, 71–77.

(22) He, M. J., Cai, W. J., Ni, W. , and Xie, L. H. RNGA-based control system configuration for multivariable processes. *J. Process Control* **2008**, submitted.

(23) Bristol, E. H. On a New Measure of Interactions for Multivariable Process Control. *IEEE Trans. Autom. Control* **1966**, *11*, 133–134.

(24) Witcher, M.; McAvoy, T. J. Interacting control systems: steady state and dynamic measurement of interactions. *ISA Trans.* **1977**, *16*, 35–41.

(25) McAvoy, T. J.; Arkun, Y.; Chen, R.; Robinson, D.; Schnelle, P. D. A new approach to defining a dynamic relative gain. *Control Eng. Pract.* **2003**, *11*, 907–914.

(26) Luyben, W. L. Simple method for tuning SISO controllers in multivariable systems. *Ind. Eng. Chem. Proc. Des. Dev.* **1986**, *25*, 654–660.

(27) Wang, Y. G.; Cai, W. J. Advanced Proportional-Integral-Derivative Tuning for Integrating and Unstable Processes with Gain and Phase Margin Specifications. *Ind. Eng. Chem. Res.* **2002**, *41*, 2910–2914.

Received for review April 17, 2008
Revised manuscript received June 22, 2008
Accepted July 14, 2008

IE8006165